

# Hadron Physics and the Dyson–Schwinger Equations of QCD

Pieter Maris

*Dept. of Physics and Astronomy, University of Pittsburgh, Pittsburgh, PA 15260*

**Abstract.** We use the Bethe–Salpeter equation in rainbow-ladder truncation to calculate the ground state mesons from the chiral limit to bottomonium, with an effective interaction that was previously fitted to the chiral condensate and pion decay constant. Our results are in reasonable agreement with the data, as are the vector and pseudoscalar decay constants. The meson mass differences tend to become constant in the heavy-quark limit. We also present calculations for the pion and rho electromagnetic form factors, and for the single-quark form factors of the  $\eta_c$  and  $J/\psi$ .

**Keywords:** Bethe–Salpeter equation, meson, quark propagator, electromagnetic form factor

**PACS:** 11.10.St, 12.38.Lg, 13.40.Gp, 14.40.-n

## INTRODUCTION

Hadrons are color-singlet bound states of quarks, antiquarks, and gluons. Bound states appear as poles in the  $n$ -point functions of a quantum field theory. Thus a study of the poles in the  $n$ -point functions of QCD will tell us something about hadrons.

In the ultraviolet region, these  $n$ -point functions can be calculated using perturbation theory. For hadronic observables however, we need to understand the nonperturbative, infrared behavior of the  $n$ -point functions of QCD. The Dyson–Schwinger equations [DSEs], which are the equations of motion of a quantum field theory, provide us with a tool to study the  $n$ -point functions nonperturbatively. For reviews on the DSEs and their use in hadron physics, see [1, 2, 3, 4, 5].

## MESON PHYSICS

Mesons can be described by solutions of the homogeneous Bethe–Salpeter equation

$$\Gamma(p_{\text{out}}, p_{\text{in}}; P) = \int \frac{d^4k}{(2\pi)^4} K(p_{\text{out}}, p_{\text{in}}; k_{\text{out}}, k_{\text{in}}) \chi(k_{\text{out}}, k_{\text{in}}; P), \quad (1)$$

with  $p_{\text{in}}$ ,  $p_{\text{out}}$  the 4-momenta of the quark and antiquark, subject to momentum conservation:  $p_{\text{in}} - p_{\text{out}} = P$ ,  $\Gamma$  the Bethe–Salpeter amplitude [BSA], and  $\chi(k_{\text{out}}, k_{\text{in}}; P) = S(k_{\text{out}}) \Gamma(k_{\text{out}}, k_{\text{in}}; P) S(k_{\text{in}})$ ; the kernel  $K$  is the  $q\bar{q}$  scattering kernel. This integral equation has solutions  $\Gamma$  at discrete values of  $P^2 = -M^2$  (in Euclidean metric) of the total meson 4-momentum  $P$ . Different types of mesons, such as pseudoscalar or vector mesons, are characterized by different Dirac structures. The properly normalized BSA  $\Gamma(p_{\text{out}}, p_{\text{in}}; P)$  completely describes the meson as a  $q\bar{q}$  bound state.

Since Eq. (1) has solutions at discrete values of  $P^2 = -M_i^2$ , one does not obtain the “complete” spectrum, including the excited states, by solving a matrix equation once; instead, one has to repeatedly solve Eq. (1) at different values of  $P^2$  in order to find the mass spectrum. The ground state in any particular spin-flavor channel corresponds to the solution with the lowest mass,  $M_0$ . Excited states can be found by looking for solutions of Eq. (1) with a larger mass  $M_i > M_0$ , and this can indeed be done [6, 7].

## Rainbow-ladder truncation

A viable truncation of the infinite set of DSEs has to respect relevant (global) symmetries of QCD such as chiral symmetry, Lorentz invariance, and renormalization group invariance. Here we use the so-called rainbow-ladder truncation, in which the  $q\bar{q}$  scattering kernel is replaced by an effective one-gluon exchange

$$K(p_{\text{out}}, p_{\text{in}}; k_{\text{out}}, k_{\text{in}}) \rightarrow -4\pi\alpha(q^2) D_{\mu\nu}^{\text{free}}(q) \frac{\lambda^i}{2} \gamma_\mu \otimes \frac{\lambda^i}{2} \gamma_\nu, \quad (2)$$

where  $q = p_{\text{out}} - k_{\text{out}} = p_{\text{in}} - k_{\text{in}}$ , and  $\alpha(q^2)$  is an effective running coupling. The corresponding truncation of the quark DSE is

$$S(p)^{-1} = i \not{p} Z_2 + m_q(\mu) Z_4 + \frac{4}{3} \int \frac{d^4 k}{(2\pi)^4} 4\pi\alpha(q^2) D_{\mu\nu}^{\text{free}}(q) \gamma_\mu S(k) \gamma_\nu, \quad (3)$$

where  $S(p) = Z(p^2)/[i \not{p} + M(p^2)]$  and  $q = k - p$ . This truncation is the first term in a systematic expansion [8] of the quark-antiquark scattering kernel  $K$ ; asymptotically, it reduces to leading-order perturbation theory. Furthermore, these two truncations are mutually consistent in the sense that the combination produces vector and axial-vector vertices satisfying their respective Ward identities.

For the effective interaction we use the 2-parameter model of Ref. [10]

$$\frac{4\pi\alpha(q^2)}{k^2} = \frac{4\pi^2 D k^2}{\omega^6} e^{-k^2/\omega^2} + \frac{4\pi^2 \gamma_m \mathcal{F}(k^2)}{\frac{1}{2} \ln \left[ e^2 - 1 + (1 + k^2/\Lambda_{\text{QCD}}^2)^2 \right]}, \quad (4)$$

with  $\mathcal{F}(s) = (1 - e^{-s})/s$ ,  $\gamma_m = 12/(33 - 2N_f)$ , and fixed parameters  $N_f = 4$  and  $\Lambda_{\text{QCD}} = 0.234 \text{ GeV}$ . The remaining parameters,  $\omega = 0.4 \text{ GeV}$  and  $D = 0.93 \text{ GeV}^2$ , were fitted in [10] to reproduce a chiral condensate of  $(240 \text{ MeV})^3$  and  $f_\pi = 131 \text{ MeV}$ . The first term in Eq. (4) models the infrared enhancement of the effective  $q\bar{q}$  scattering kernel necessary to generate the experimentally observed amount of dynamical chiral symmetry breaking [11]. It was introduced in [10] as a finite-width representation of a  $\delta$ -function [12], which can be interpreted as a regularized  $1/p^4$  singularity in  $K$  [13, 14]. The second term ensures the correct perturbative behavior in the ultraviolet region.

## Meson spectroscopy

In Table 1 we give our results for the equal-mass ground states in each spin channel. The masses of the light quarks were fitted in [10] to the pion mass (using equal  $u$  and  $d$  quark masses) and to the kaon mass. The light vector and pseudoscalar mesons are described very well by this model: not only their masses, but also a wide range of other observables agree with experiments, without adjusting any of the parameters, see [4] and references therein. Here we apply this model to heavy quarks as well, and use the vector mesons  $J/\psi$  and  $\Upsilon$  to fix the  $c$  and  $b$  masses.

The mass splitting between the pseudoscalar and vector mesons is too large for the heavy quarkonium states, but the decay constants are in reasonable agreement with available data. On the other hand, the mass splitting between the vector and the scalar mesons is too small; and the scalar-pseudoscalar mass difference is reasonable. Also the axialvector masses are too small, but the mass difference between the scalar and the  $1^{++}$  states is in agreement with data, both for the light and for the  $c$  and  $b$  quarks. Similar results for the light quark sector and for the charmonium states were found in Ref. [17] with a slightly different model interaction. Presumably corrections beyond ladder truncation are necessary for the scalar and axialvector masses: there are significant cancellations between these corrections in the pseudoscalar and vector channels [8], but not necessarily in the scalar and axialvector channels.

Over the entire mass range from the chiral limit up to the bottomonium states, the pseudoscalar, vector, and scalar masses can be fitted by

$$M_{\text{meson}}^2 = C_0 + C_1 m_q + C_2 m_q^2, \quad (5)$$

where  $m_q$  is the current quark mass at our renormalization point  $\mu = 19$  GeV. The fit parameters are  $C_0 = 0$  and  $C_1 = 6.94$  for the pseudoscalars,  $C_0 = 0.51$  and  $C_1 = 7.27$  for the vectors, and  $C_0 = 0.38$  and  $C_1 = 8.65$  for the scalar mesons, with a common parameter  $C_2 \approx 4.6$ . The fact that the trajectories can all be fitted with (approximately) the same value for  $C_2$  means that for large masses, the meson mass differences become constant: in the limit  $m_q \rightarrow \infty$  the above fit suggests  $\Delta M \rightarrow \frac{1}{2}\Delta C_1/\sqrt{C_2}$ . Thus this global fit indicates that the mass difference  $M_V - M_{\text{PS}}$  approaches 0.07 GeV, whereas  $M_S - M_{\text{PS}}$  approaches 0.4 GeV for heavy quarks; our numerical results however do not exclude that

**TABLE 1.** Masses and leptonic decay constants for equal-mass ground state  $J^{PC}$  mesons. Experimental data are from Ref. [15], with the exception of  $f_{\eta_c}$  [16].

quark flavor	$M_{\text{PS}}$	$f_{\text{PS}}$	$M_V$	$f_V$	$M(0^{++})$	$M(1^{+-})$	$M(1^{++})$
up/down	0.1385	0.131	0.743	0.207	0.672	0.83	0.91
expt.	0.135, 0.140	0.131	0.775	0.221	0.985	1.23	1.23
strange	0.697	0.183	1.076	0.260	1.081	1.17	1.25
expt.	—	—	1.020	0.229	—	—	—
charm	2.908	0.381	3.098	0.421	3.250	3.26	3.33
expt.	2.980	$0.335 \pm 0.075$	3.097	0.416	3.415		3.51
bottom	9.38	0.66	9.46	0.62	9.72	9.73	9.75
expt.	9.30		9.46	0.715	9.86		9.89

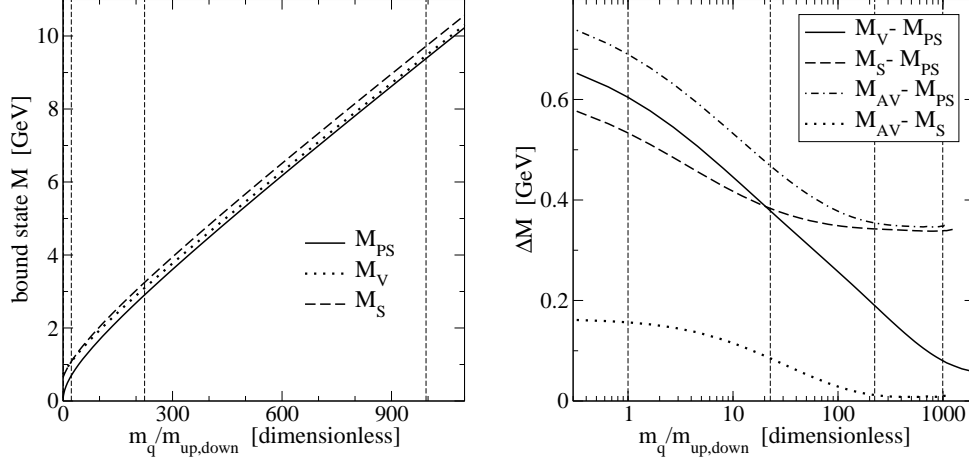


**FIGURE 1.** Meson masses (left) and mass differences (right) as function of current quark mass, normalized to the up and down quark masses. The vertical dashed lines indicate physical quark masses.

the coefficients  $C_1$  are identical for the pseudoscalar and vector mesons, in which case this mass difference vanishes in the heavy quark limit.

This is indeed consistent if we look at the actual mass differences we find, see the right panel of Fig. 1: the mass difference  $M_V - M_{PS}$  decreases with increasing quark mass, it is about  $\Delta_M \approx 0.06$  GeV for at  $2m_b$ , and still decreasing. Similarly, the mass difference  $M_{AV} - M_S$  appears to vanish in the heavy quark limit, but the differences  $M_S - M_{PS}$  and  $M_{AV} - M_{PS}$  clearly remain nonzero and appear to go to a constant of about  $\Delta M \approx 0.35$  GeV. However, one should keep in mind that the model was fitted to the pion decay constant and the chiral condensate; implicitly we may have incorporated corrections beyond the ladder kernel in our model for the effective  $q\bar{q}$  scattering kernel. Higher-order corrections affect light quarks differently than heavy quarks [9].

The corresponding quark mass functions are shown in Fig. 2, and summarized in Table 2. Our current quark masses are in good agreement with conventional values [15] of both the light and the heavy quark masses. For the light quarks, the nonperturbative mass function  $M_q(p^2)$  is significantly larger than the perturbative quark mass  $m_q(\mu)$  at  $p = 2 = \mu$ , indicating that chiral symmetry breaking sets in well above this scale. The momentum dependence of  $M_{c,b}(p^2)$  is much less dramatic. Nevertheless, there is a

**TABLE 2.** Current quark masses  $m_q(\mu)$  at  $\mu = 19$  GeV, scaled down to  $\mu = 2$  GeV and to  $\mu = m_q$  using one-loop pQCD, together with the dynamical mass function  $M(p^2)$  at several values of  $p^2$ .

$m_q(19)$	$m_q(2)$	$m_q(m_q)$	$M_q(p^2 = M_q(p^2)^2)$	$M_q(p^2 = 4)$	$M_q(p^2 = 0)$	$M_q(p^2 = -\frac{1}{4}M_V^2)$
chiral limit			0.392	0.010	0.477	0.594
0.0037	0.005		0.401	0.017	0.499	0.610
0.0838	0.118		0.556	0.168	0.689	0.845
0.827	1.17	1.30	1.42	1.31	1.61	2.00
3.68	5.65	4.46	4.30	4.46	4.52	5.33

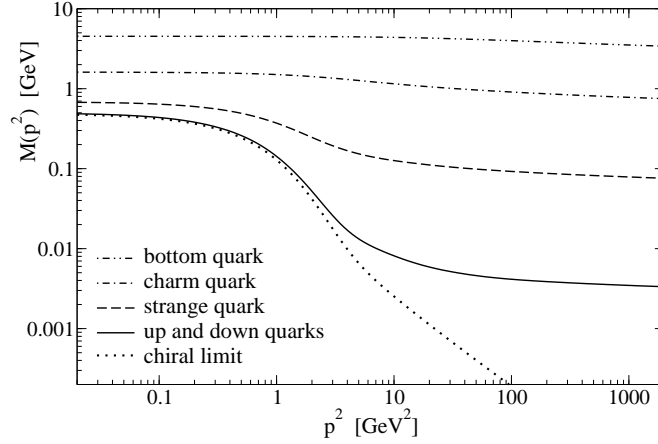


**FIGURE 2.** Dynamical quark mass function  $M_q(p^2)$  for  $u = d, s, c, b$  and chiral quarks.

significant difference between the dynamical mass in the region relevant for  $q\bar{q}$  bound states, namely  $p^2 \sim -\frac{1}{4}M_{\text{meson}}^2$  in the timelike region, and  $M_{c,b}(p^2)$  in the spacelike region, even for  $b$  quarks. For  $0 < p^2 < -\frac{1}{4}M_{\text{meson}}^2$ , the mass function of the heavy quarks is in fact quite close to the typical pole masses used in non-relativistic calculations of charmonium,  $m_c^{\text{pole}} \approx 1.47$  to  $1.83$  GeV and bottomonium,  $m_b^{\text{pole}} \approx 4.7$  to  $5.0$  GeV [15].

## Electromagnetic form factors

The  $q\bar{q}\gamma$  vertex is the solution of the renormalized inhomogeneous Bethe–Salpeter equation with the same kernel  $K$  as Eq. (1). Thus for photon momentum  $Q$ , we have

$$\Gamma_\mu(p_{\text{out}}, p_{\text{in}}) = Z_2 \gamma_\mu + \int \frac{d^4k}{(2\pi)^4} K(p_{\text{out}}, p_{\text{in}}; k_{\text{out}}, k_{\text{in}}) S(k_{\text{out}}) \Gamma_\mu(k_{\text{out}}, k_{\text{in}}) S(k_{\text{in}}), \quad (6)$$

with  $p_{\text{out}}$  and  $p_{\text{in}}$  the outgoing and incoming quark momenta, respectively, and similarly for  $k_{\text{out}}$  and  $k_{\text{in}}$ , with  $p_{\text{out}} - p_{\text{in}} = k_{\text{out}} - k_{\text{in}} = Q$ . The ladder truncation for Eq. (6), in combination with the rainbow truncation for the quark propagators and impulse approximation for electromagnetic form factors, satisfies the vector Ward–Takahashi identity and electromagnetic current conservation is guaranteed.

Also note that solutions of the *homogeneous* version of Eq. (6) define vector meson bound states with masses  $M_V^2 = -Q^2$  at discrete timelike momenta  $Q^2$ . It follows that  $\Gamma_\mu$  has poles at those locations. Thus the effects of intermediate vector meson states on electromagnetic processes can be unambiguously incorporated by using the properly dressed  $q\bar{q}\gamma$  vertex rather than the bare vertex  $\gamma_\mu$  [18].

Consider for example the 3-point function describing the coupling of a photon with momentum  $Q$  to the quark  $a$  of a meson  $a\bar{b}$ , with initial and final momenta  $P \pm \frac{1}{2}Q$

$$\Lambda_\mu^a(P, Q) = iN_c \int \frac{d^4k}{(2\pi)^4} \text{Tr}[\Gamma_\mu^a(q_-, q_+) \chi^{a\bar{b}}(q_+, q) S^b(q)^{-1} \bar{\chi}^{\bar{b}a}(q, q_-)] , \quad (7)$$

**TABLE 3.** Static electromagnetic properties of pseudoscalar and vector  $u\bar{d}$  mesons ( $\pi$  and  $\rho$ ) and  $c\bar{c}$  mesons (fictitious).

	$r_{\text{PS}}^2$	$r_{\text{V,E}}^2$	$\mu$	$r_{\text{V,M}}^2$	$\mathcal{Q}$
up/down	0.44	0.54	2.01	0.49	-0.41
charm	0.048	0.052	2.13	0.047	-0.28
lattice [23]	0.063(1)	0.066(2)	2.10(3)		-0.23(2)

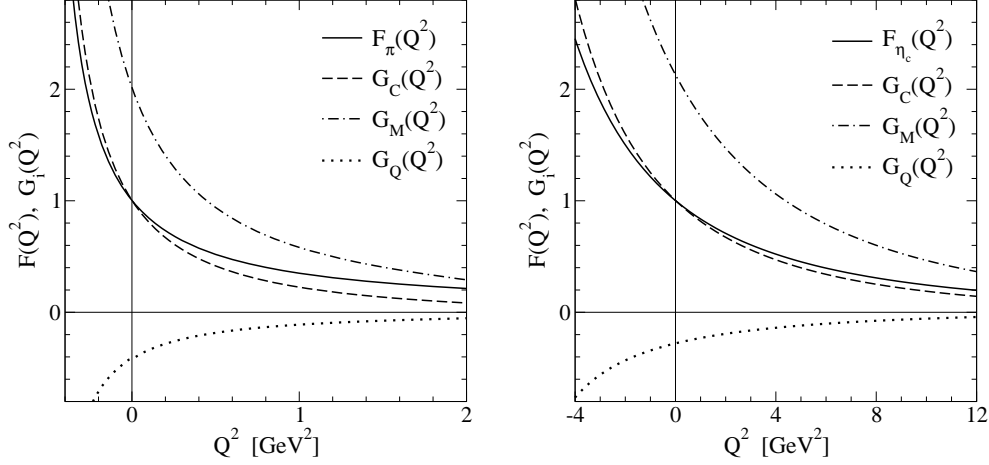


**FIGURE 3.** Single-quark form factors:  $\pi$  and  $\rho$  (left) and  $c\bar{c}$  pseudoscalar and vector mesons (right).

with  $q = k - \frac{1}{2}P$  and  $q_{\pm} = k + \frac{1}{2}P \pm \frac{1}{2}Q$ . The corresponding single-quark elastic form factor  $F^a$  of a pseudoscalar meson is defined by

$$2 P_{\mu} F^a(Q^2) = \Lambda_{\mu}^a(P, Q). \quad (8)$$

Vector mesons have three elastic form factors, commonly referred to as the electric, magnetic, and quadrupole form factors  $G_E(Q^2)$ ,  $G_M(Q^2)$ , and  $G_Q(Q^2)$ . The electric monopole moment (i.e. the electric charge), magnetic dipole moment and the electric quadrupole moment follow from the values of these form factors in the limit  $Q^2 \rightarrow 0$ :  $G_E(0) = 1$  (constrained by current conservation),  $G_M(0) = \mu$ , and  $G_Q(0) = \mathcal{Q}$ .

Our results for the pion form factor [18, 19] are in good agreement with the data, both in the spacelike region [20] and in the timelike region; the charge radius agrees very well with the experimental value  $\langle r_{\pi}^2 \rangle = 0.44 \pm 0.01 \text{ fm}^2$  [21], see Table 3. The vector charge radius [22] is slightly larger than the pseudoscalar radius, both for light quarks and for charm quarks. This suggests that the vector states are broader than the corresponding pseudoscalar states, assuming that the charge distribution is indicative of the physical size of the bound state. This agrees with the naive intuition that a more tightly bound state is more compact than a heavier state with the same constituents. For charm quarks this difference is significantly smaller than for up and down quarks, in agreement with recent lattice calculations [23]. The magnetic moment appears to be surprisingly independent of the quark mass; the quadrupole moment decreases with

increasing quark mass [22]. Recent lattice simulations [23] agree quite well with our results for the moments of the single-quark form factors of the  $J/\psi$ .

In Fig. 3 we see that both the pseudoscalar  $F_\pi$  and all three vector form factors  $G_i^\rho$  diverge in the timelike region as  $Q^2 \rightarrow -0.55 \text{ GeV}^2$ , corresponding to the vector-meson poles in the dressed quark photon vertex. Similarly, the single-quark form factors of the  $\eta_c$  and  $J/\psi$  diverge as  $Q^2 \rightarrow -9.5 \text{ GeV}^2$ . However, it is only the pion form factor that can be described by a vector meson dominance [VMD] curve,  $F_\pi \approx M_\rho^2/[Q^2 + M_\rho^2]$ , over the entire  $Q^2$ -region shown. The  $\rho$  form factors  $G_i^\rho$  drop significantly faster [22] than a VMD curve, as do the  $c\bar{c}$  form factors, both for pseudoscalar and vector states.

## ACKNOWLEDGMENTS

This work was supported by the US Department of Energy, contract No. DE-FG02-00ER41135, and benefited from the facilities of the NSF Terascale Computing System at the Pittsburgh Supercomputing Center.

## REFERENCES

1. C.D. Roberts and A.G. Williams, Prog. Part. Nucl. Phys. **33**, 477 (1994) [arXiv:hep-ph/9403224].
2. C.D. Roberts and S.M. Schmidt, Prog. Part. Nucl. Phys. **45S1**, 1 (2000) [arXiv:nucl-th/0005064].
3. R. Alkofer and L. von Smekal, Phys. Rept. **353**, 281 (2001) [arXiv:hep-ph/0007355].
4. P. Maris and C.D. Roberts, Int. J. Mod. Phys. E **12**, 297 (2003) [arXiv:nucl-th/0301049].
5. C.S. Fischer, J. Phys. G **32**, R253 (2006) [arXiv:hep-ph/0605173].
6. A. Holl, A. Krassnigg and C.D. Roberts, Phys. Rev. C **70**, 042203 (2004) [arXiv:nucl-th/0406030].
7. A. Holl *et al.*, Phys. Rev. C **71**, 065204 (2005) [arXiv:nucl-th/0503043].
8. A. Bender, C.D. Roberts and L. Von Smekal, Phys. Lett. B **380**, 7 (1996) [arXiv:nucl-th/9602012]; A. Bender *et al.*, Phys. Rev. C **65**, 065203 (2002) [arXiv:nucl-th/0202082].
9. M.S. Bhagwat, A. Holl, A. Krassnigg, C.D. Roberts and P.C. Tandy, Phys. Rev. C **70**, 035205 (2004) [arXiv:nucl-th/0403012].
10. P. Maris and P.C. Tandy, Phys. Rev. C **60**, 055214 (1999) [arXiv:nucl-th/9905056].
11. F.T. Hawes, P. Maris and C.D. Roberts, Phys. Lett. B **440**, 353 (1998) [arXiv:nucl-th/9807056].
12. P. Maris and C.D. Roberts, Phys. Rev. C **56**, 3369 (1997) [arXiv:nucl-th/9708029].
13. D.W. McKay and H.J. Munczek, Phys. Rev. D **55**, 2455 (1997) [arXiv:hep-th/9607075].
14. R. Alkofer, C.S. Fischer and F.J. Llanes-Estrada, arXiv:hep-ph/0607293.
15. W. M. Yao *et al.* [Particle Data Group], J. Phys. G **33**, 1 (2006).
16. K.W. Edwards *et al.* [CLEO Collaboration], Phys. Rev. Lett. **86**, 30 (2001) [arXiv:hep-ex/0007012].
17. R. Alkofer, P. Watson and H. Weigel, Phys. Rev. D **65**, 094026 (2002) [arXiv:hep-ph/0202053].
18. P. Maris and P.C. Tandy, Phys. Rev. C **61**, 045202 (2000) [arXiv:nucl-th/9910033].
19. P. Maris and P.C. Tandy, Phys. Rev. C **62**, 055204 (2000) [arXiv:nucl-th/0005015].
20. V. Tadevosyan *et al.* [Fpi-1 Collaboration], arXiv:nucl-ex/0607007; T. Horn *et al.* [Fpi2 Collaboration], arXiv:nucl-ex/0607005.
21. S. R. Amendolia *et al.* [NA7 Collaboration], Nucl. Phys. B **277**, 168 (1986).
22. M.S. Bhagwat and P. Maris, in preparation.
23. J.J. Dudek, R.G. Edwards and D.G. Richards, Phys. Rev. D **73**, 074507 (2006) [arXiv:hep-ph/0601137].